High-Resolution Infrared Studies of Al(BH$_4$)$_3$ and Al(BD$_4$)$_3$

Abdullah Al-Kahtani, Darren L. Williams, and Joseph W. Nibler*

Department of Chemistry, Oregon State University, Corvallis, Oregon 97331

Steven W. Sharpe

William A. Wiley Environmental Molecular Science Laboratory, Pacific Northwest National Laboratory, Richland, Washington 99352

High-resolution (0.01 cm^{-1}) FTIR spectra of Al(BH$_4$)$_3$ and Al(BD$_4$)$_3$ recorded for low-pressure samples at room temperature are presented that show only broad vibrational bands, with no trace of resolved rotational structure. The BH bridge stretching and the BH$_2$ deformation regions were also examined at 0.001 cm^{-1} resolution by tunable infrared diode laser spectroscopy for samples cooled to ~10 K in a multipass, slit expansion. These too show near continua, with much more congestion than predicted by nonrigid rotor simulations based on boron isotopic shifts, Coriolis constants, and centrifugal distortion parameters estimated from ab initio calculations. The latter indicate that a particularly low barrier, corresponding to the prismatic D_{3h} structure, separates two equivalent, lower energy D_3 forms in which the BH$_4$ units are rotated 23° about the Al−B axes. The potential energy surface for the relevant conrotary torsional coordinate is examined at the CCSD/6-311G**//MP2/6-311G** level, yielding a barrier height of 490 cm^{-1} and $v = 0$ and 1 level splittings of 0.052 and 2.7 cm^{-1}, respectively. The extreme spectral congestion observed is believed to arise primarily from splittings of the ground state and the upper vibrational levels of modes that couple to this conrotary torsional motion and to other tumbling modes of the BH$_4$ units.

Introduction

Metal borohydrides are fascinating compounds because they show a remarkable variety in bonding characteristics, ranging from ionic salts of the alkali metals (e.g., LiBH$_4$ and NaBH$_4$) to volatile covalent compounds in which hydrogen bridge bonds link boron to the metal. Among the covalent compounds, Al-(BH$_4$)$_3$ is believed to have a planar trigonal skeletal structure with double hydrogen bridges,[1,2] while Zr(BH$_4$)$_4$, U(BH$_4$)$_4$, and Hf(BH$_4$)$_4$ are all thought to have tetrahedral T_d structures with triple bridges.[3] The borohydrides are among the most volatile compounds of the latter heavy metals, a fact sometimes used in their commercial purification.

Aluminum borohydride, synthesized by Schlesinger and co-workers in 1940, was the first covalent metal borohydride molecule to be characterized structurally.[4] An electron diffraction study of the compound in the same year demonstrated that the aluminum atom was linked symmetrically to all three boron atoms, with all B−Al−B angles close to 120°.[5] The positions of the hydrogen atoms remained unclear. Two NMR studies[6,7] of liquid Al(BH$_4$)$_3$ showed that all the protons were equivalent; i.e., the exchange between bridging and terminal hydrogen positions is fast (on the NMR time scale), as has been the case for all other metal borohydrides subsequently examined. The first infrared spectrum was reported in 1949[8] and, because of the great similarity to the spectrum of diborane, was interpreted in favor of the molecular structure shown in Figure 1. Each boron atom is bonded to four hydrogen atoms, located at roughly the corners of a tetrahedron, and is connected to the aluminum atom through two hydrogen bridge bonds. The infrared study
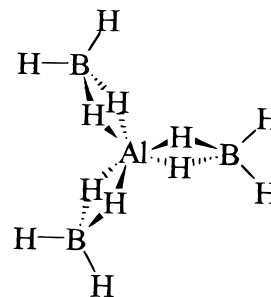
Figure 1. The D_{3h} molecular structure of aluminum borohydride, Al-(BH$_4$)$_3$. In the D_3 structure deduced from electron diffraction data,[1] the BH$_4$ units are rotated by 17°.

was consistent with a proposed prismatic D_{3h} structure in which the terminal hydrogen atoms lie in the plane of AlB$_3$ and the line joining the bridge hydrogen atoms is perpendicular to the plane. The same conclusion was also reached in a Raman study in 1960[9] on Al(^{11}BH$_4$)$_3$, Al(^{10}BH$_4$)$_3$, Al(^{11}BD$_4$)$_3$, and Al(^{10}BD$_4$)$_3$. In this study, a partial vibrational assignment was made based on a D_{3h} structure.

In 1968 another electron diffraction investigation of gaseous Al(BH$_4$)$_3$ was reported.[1] This study also showed that the aluminum and boron atoms are coplanar, with each BH$_4$ group double-bridged to the aluminum atom. However, the data could not determine conclusively the overall symmetry of the molecule. It was hypothesized that the molecule could be either of D_{3h} symmetry or of D_3 symmetry (obtained from D_{3h} by conrotation of the three BH$_2$ bridging planes). To fit the data to the last case, the rotation angle was found to be close to 17°.

The most recent vibrational investigation, reported in 1973,[2] involved detailed infrared and Raman results on gaseous, solid,

* Corresponding author. E-mail niblerj@chem.orst.edu; FAX (541) 737-2062.

538 *J. Phys. Chem. A, Vol. 102, No. 3, 1998*

Al-Kahtani et al.

TABLE 1: Geometrical Parameters of Al(BH₄)₃, in Å, deg, and cm⁻¹

Al(BH₄)₃ parameter	expt[1]	HF/ 6-31G*[11]	HF/ 6-311G**[a]	MP2/ 6-311G**[a]
Al–B	2.143	2.177	2.176	2.155
B–Hb	1.283	1.285	1.288	1.273
B–Ht	1.196	1.189	1.189	1.192
Hb–B–Hb	114.0	106.3	106.5	108.4
Ht–B–Ht	116.2	121.6	121.5	121.6
θ	17.2	23.2	23.3	23.2
$B(^{11}B_3)$	0.1475	0.1435	0.1442	0.1464
$C(^{11}B_3)$	0.0786	0.0758	0.0763	0.0775

[a] This work.

and matrix-isolated Al(BH₄)₃ and Al(BD₄)₃. It was found that there was no evidence for any significant structural change in going from the gas to solid to matrix states. Based on symmetry/selection rules, the data were found to be consistent with a D_{3h} prismatic structure, and the assignments of 23 optically allowed fundamental transitions were proposed. The assignments were found to be in satisfactory agreement with the product rule, and a number of modifications were made of the previous partial fundamental assignment.

Besides the experimental work summarized above, two ab initio investigations have been reported on the structure of Al-(BH₄)₃. In one study at the Hartree–Fock level by Bock et al.,[10] the D_{3h} and D_3 structures proposed previously were considered. A vibrational frequency analysis was performed on the prismatic D_{3h} structure to determine whether it was indeed a local potential minimum. The appearance of a single imaginary frequency showed that the D_{3h} configuration corresponded to a first-order transition state. Reducing the imposed symmetry to D_3, by allowing the BH₄ units to rotate in a conrotary fashion, lowered the energy by about 5.9 kJ mol⁻¹. A subsequent frequency analysis at the same level showed the antiprismatic D_3 structure to be a stable configuration (i.e., all vibrational frequencies were real). It was suggested that the rotation lowered the energy by reducing the Coulombic repulsion between hydridic hydrogens in each of the upper and lower prismatic planes, but the rotation angle was not given.

In a later study at a higher level of ab initio theory, Demachy et al. included electron correlation using second-order perturbation theory (MP2) and configuration interaction (CIPSI).[11] The rotational barrier associated with the conrotation of the three BH₄ groups around the Al–B bond in the bidentate structure of Al(BH₄)₃ was found to be reduced from the Hartree–Fock result of 5.9 kJ mol⁻¹ to 0.8 kJ mol⁻¹. The rotation angle (θ = 23.2°) and other structural parameters of this minimum are given in Table 1, along with the electron diffraction results.[1] It was found also that changing the coordination mode of one borohydride group from bidentate to tridentate leads to a structure that is the transition state for the exchange of bridging and terminal hydrogens. This BH₄ "tumbling" barrier was found to have a relatively low energy (9.2 kJ mol⁻¹), a result consistent with the lack of distinction between bridging and terminal hydrogens in the proton NMR spectrum. In contrast, a transition barrier of 103.8 kJ mol⁻¹ was found for the change in coordination of one borohydride group from bidentate to monodentate.

Whereas both theoretical studies support a stable D_3 geometry for Al(BH₄)₃ with facile BH₄ motion about the Al–B axes, the existing experimental data cannot distinguish between D_3 and D_{3h} forms. The calculated rotational constants (Table 1) suggest that the 2B line separation in the infrared P and R branches should be about 0.3 cm⁻¹, not resolvable at the resolution of

previous studies but well within the capability of current instruments. Of course, because the structural change from D_{3h} to D_3 is slight, it is not likely that measurements of the rotational constants would distinguish between these forms. In principle, a distinction might be possible from rotationally resolved $K =$ 0 line intensities although this too is problematic since the variation will be quite small. Moreover, one might also expect some subtle splittings of lines and intensity perturbations due to torsional and tumbling rotations of the BH₄ units. If measurable, the latter splittings are in fact of special interest because they are governed by the transition barriers for motions on the potential energy surface. Accordingly, in the present work we have sought such vibration–rotational fine structure for Al(BH₄)₃ and Al(BD₄)₃ using FTIR and IR diode laser spectroscopy at a resolution down to 0.001 cm⁻¹. The results of these studies, along with some further ab initio calculations, are presented here.

Experimental Section

Al(BH₄)₃ was prepared via the solid-state metathetic reaction of aluminum chloride and lithium borohydride, following the method of Schlesinger et al.[12] Because of the pyrophoric nature of the molecule, all reactants were handled in a dry bag, and the reaction was carried out in a hood using a greaseless vacuum system. In the dry bag, 1 g of anhydrous AlCl₃ (99.5%, Aldrich Inc.) and 4 g of anhydrous sodium borohydride (95%, Alfa) were mixed in a reaction tube. This was then attached to a vacuum line, evacuated, and then slowly heated over 8 h to 140 °C while pumping volatile Al(BH₄)₃ and B₂H₆ products through a condensation trap at 77 K. The diborane was subsequently removed by warming the trap to about 200 K while pumping. Al(BD₄)₃ was made by the analogous reaction of AlCl₃ with NaBD₄ and purified by a similar procedure.

Survey infrared spectra were recorded using a Mattson Sirius 100 FTIR spectrometer, which has a resolution of 0.125 cm⁻¹. Samples at 5–10 Torr pressure were placed in 10 or 20 cm cells equipped with KBr windows. No rotationally resolved structure was seen in the spectra so higher resolution infrared spectra (0.01 cm⁻¹) were then recorded at Pacific Northwest National Laboratories (PNNL) using a Bruker IFS 120 HR FTIR spectrometer. The Al(BH₄)₃ region near 2100 cm⁻¹ was also examined at 0.001 cm⁻¹ resolution using an IR diode laser and a multipass gas cell at PNNL.

Finally, infrared diode-laser spectra of Al(BH₄)₃ cooled in a jet were collected, using a special spectrometer system developed at PNNL.[13] This consists of a Laser Photonics cold head mounted on an optical table and containing up to four laser diodes. The output of a selected diode is collimated and directed into a 0.5 m monochromator, the output of which is intercepted by a rotating gold-coated aluminum sector. The sector intercepts and directs the laser light one-third of the time to a reference cell, one-third of the time to a 0.25 m confocal etalon, and the rest of the time into the vacuum chamber where it intercepts the effluent of a pulsed slit nozzle of 100 mm length. Laser light entering the vacuum chamber through BaF₂ windows is multipassed up to 32 times through the supersonic jet, using a White cell optical configuration. The signals from the three InSb detectors are fed into three parallel digitizers that sample 4096 points at 200 ns intervals, yielding a spectral scan of about 0.4 cm⁻¹. The pulsed valve and the three digitizers are synchronized with the angular position of the rotating sector using a microprocessor, and signal averaging is done by real-time, coaddition of individual spectra over 5–10 gas pulses.
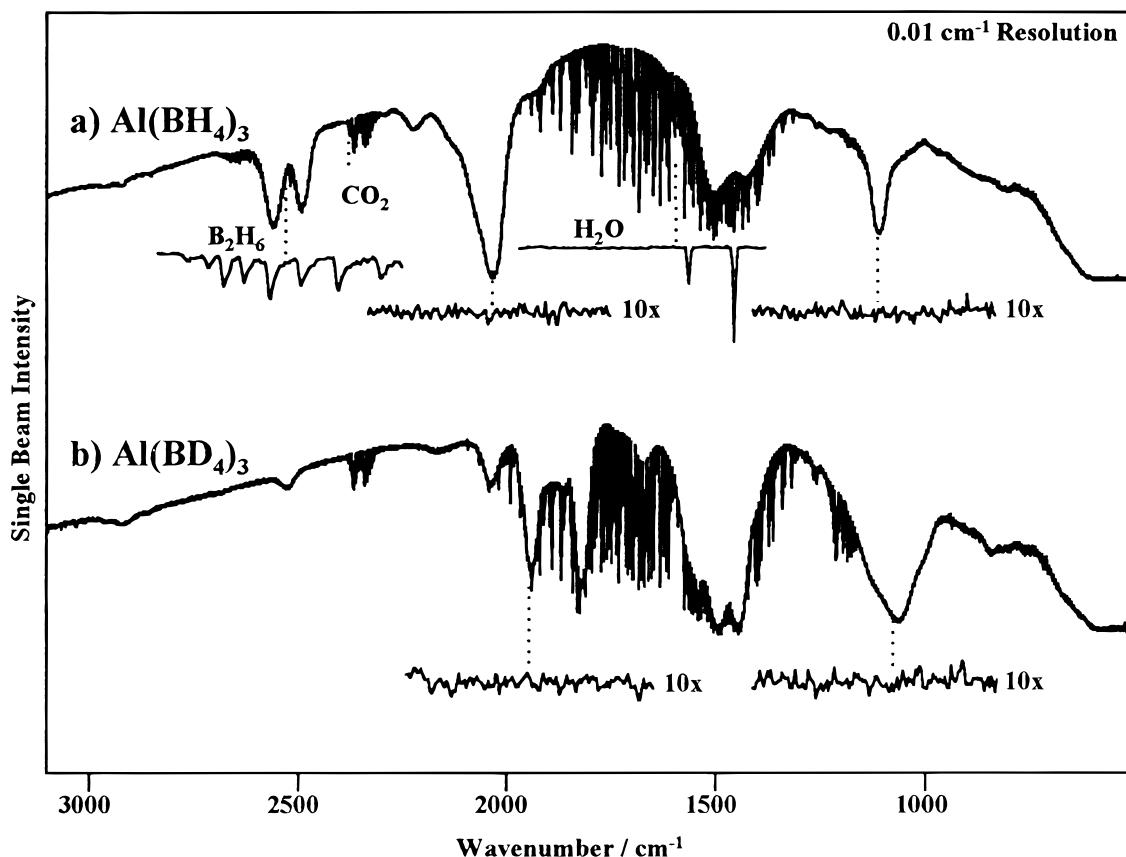
Figure 2. FTIR of (a) Al(BH$_4$)$_3$ and (b) Al(BD$_4$)$_3$ at 0.01 cm^{-1} resolution. The 1 cm^{-1} expanded regions show resolved rovibrational structure for background H$_2$O and B$_2$H$_6$ contaminant. No such structure was seen for Al(BH$_4$)$_3$ or Al(BD$_4$)$_3$, even at 10× ordinate expansion.

Results and Discussion

FTIR Spectra of Al(BH$_4$)$_3$ and Al(BD$_4$)$_3$. A spectrum recorded at 0.010 cm^{-1} resolution for 6 Torr of Al(BH$_4$)$_3$ in a 10 cm cell is shown in the top trace of Figure 2. Broad regions of absorption by Al(BH$_4$)$_3$ are seen in these single-beam spectra, along with sharp features of diborane contaminant in the sample and of residual CO$_2$ and H$_2$O in the evacuated FTIR instrument. The 1 cm^{-1} expanded portions of several of the major features are given as inserts in the figure. The sharp features in the top trace at 2520 cm^{-1} and the bottom trace at 1200 cm^{-1} can be positively identified as diborane lines. The line width of these (0.016 cm^{-1} fwhm) establishes the limiting measurement resolution, which is due to the convolution of the instrumental resolution, the Doppler width (about 0.005 cm^{-1}), and the collisional width (estimated to be <0.002 cm^{-1}). The Doppler width for Al(BH$_4$)$_3$ is about 0.003 cm^{-1}, and the collisional broadening in this nonpolar molecule is likely to be comparable to that in diborane.

At our measurement resolution one would expect to easily resolve P and R rotational lines with spacings of about 0.3 cm^{-1}. The P−Q−R band contours for parallel modes of A$_2''$ symmetry should be distinguishable, with a P−R maxima separation of about 16 cm^{-1} at room temperature. For E′ perpendicular bands, strong Q branch maxima spaced by 2(C−B) $\sim$ 0.15 cm^{-1} are expected. Some blurring of these predictions will of course result from K splittings and Coriolis and centrifugal distortion effects. However, the expanded traces at 2020 and 1100 cm^{-1} (top, Al(BH$_4$)$_3$) and 1990 and 1050 cm^{-1} (bottom, Al(BD$_4$)$_3$) show no hint whatsoever of resolved rotational structure. Moreover, several diode laser scans at 0.001 cm^{-1} resolution for room-temperature Al(BH$_4$)$_3$ at low pressures confirmed the essentially continuous absorption in the region near 2030 cm^{-1}.

The broad features in the traces are the same as those reported for Al(BH$_4$)$_3$ and Al(BD$_4$)$_3$ in ref 2 and in none of the spectra are P−Q−R band contours discernible. It should also be noted that the increased mass of the BD$_4$ did not reduce the spectral congestion, as might have been expected if splittings due to rotational tunneling between potential minima were the major cause of spectral complexity.

Isotopic Contributions to Spectral Congestion. The complete absence of any resolved rotational structure in the vibrational spectra of Al(BH$_4$)$_3$, even at 0.001 cm^{-1} resolution, was surprising but might be a consequence of overlap of bands due to the different boron isotopic forms and to hot bands involving low-lying vibrational levels. The isotopic forms for Al(BH$_4$)$_3$ are ^{11}B$_3$ (51%), ^{11}B$_2^{10}$B (38%), ^{11}B^{10}B$_2$ (10%), and ^{10}B$_3$ (1%); we neglected the contribution of the latter two minor forms in the spectral simulations described here. The ^{10}B vibrational shift will vary for different modes, and these were predicted from Gaussian calculations done at the Hartree−Fock level with a 6-311G** basis set. Frequencies and intensities for the ^{11}B$_3$ form are listed in Table 2, with the former scaled by about 0.9 according to common practice.[14]

Band spectra were simulated for three vibrational fundamentals predicted by Gaussian to have high infrared intensities. One of these was the E′ terminal BH$_2$ bending deformation, a perpendicular band near 1110 cm^{-1} assigned by Coe et al.[2] as ν_{19}. For the ^{11}B$_2^{10}$B form, the calculations show that this degenerate E mode yields two uncoupled modes: one at the same wavenumber value as in the ^{11}B$_3$ compound and a second ^{10}B mode 4.1 cm^{-1} higher and with equal intensity. A similar uncoupling was calculated for the E′ bridge stretching mode near 2020 cm^{-1}, but with a smaller ^{10}B−^{11}B shift of 1.1 cm^{-1}. The A$_2''$ symmetric counterpart of this bridge stretch, a parallel

TABLE 2: Wavenumbers and Infrared Intensities (km mol^{-1}) Calculated for the Vibrational Fundamentals of Al(BH$_4$)$_3$ Using Gaussian at the HF/6-311G Level**

HF/6-311G**			experimental[2]		
D_3	ω^a	IR int	ω	D_{3h}	mode desc
A$_1$	2368		2471	A$_1'$	BH$_t$ st sym
E	2364	96	2490	E$'$	BH$_t$ st sym
A$_2$	2439	52		A$_2'$	BH$_t$ st asym
E	2441	145	2555	E$'$	BH$_t$ st asym
A$_1$	1928		2059	A$_1'$	BH$_b$ st sym
E	**1874**	**561**	**2059**^{b}	**E$'$**	**BH$_b$ st sym**^{c}
A$_2$	**1915**	**336**	**2030**^{b}	**A$_2''$**	**BH$_b$ st asym**^{c}
E	1789	55	2030	E$''$	BH$_b$ st asym
A$_1$	1544		1511	A$_1'$	AlH$_b$ st sym
E	1353	7	1425	E$'$	AlH$_b$ st sym
A$_2$	1385	42	1505	A$_2''$	AlH$_b$ st asym
E	1501	616	1565	E$''$	AlH$_b$ st asym
A$_1$	1112			A$_1''$	BH$_2$ twist
E	1107	3	1155	E$''$	BH$_2$ twist
A$_1$	1102			A$_1''$	bridge twist
E	994	27	1146	E$''$	bridge twist
A$_2$	986	5	1113	A$_1'$	BH$_2$ def
E	**1097**	**129**	**1112**	**E$'$**	**BH$_2$ def**^{c}
A$_2$	776	6		A$_2'$	BH$_2$ rock xy
E	713	0.2	981	E$'$	BH$_2$ rock xy
A$_1$	443		765	A$_2''$	BH$_2$ wag z
E	550	117	723	E$''$	BH$_2$ wag z
A$_1$	228		495	A$_1'$	AlB st sym
E	376	18	605	E$'$	AlB st asym
A$_2$	167	18	222	A$_2''$	B$_3$ bend z
E	253	0.04	324	E$'$	B$_3$ bend xy
A$_2$	263	6		A$_2'$	bridge bend
E	116	10	255	E$'$	bridge bend

^{a} Wavenumber values scaled by 0.8929 as recommended in ref 14. ^{b} The calculated transitions and intensities favor the reversal of these two wavenumber assignments. ^{c} Transitions studied by diode laser in this work are bolfaced.

band, was predicted by the Gaussian calculation to lie 41 cm^{-1} higher than the E$'$ mode and to have a ^{10}B$-^{11}$B shift of 2.6 cm^{-1}. We note that this ordering is a reversal of that chosen by Coe et al.,[2] who assigned the intense infrared peaks near 2030 and 2056 cm^{-1} as A$_2''$(ν_{11}) and E$'$(ν_{17}), respectively. The basis for their assignment was not strong, however, and the match of the calculated intensities to the FTIR data favors the A$_2''$ > E$'$ ordering adopted in our simulations. In general, the calculated ^{10}B shifts are comparable to those observed experimentally for similar modes in diborane.

Simulations of both parallel and perpendicular band spectra were done with Grams/32[15] using Array Basic and standard relations given in ref 16; the ^{11}B$_2$^{10}B isotopic form was taken to be a near-oblate top with averaged rotational constant ($A + B$)/2. The band origins of the two E$'$ modes were adjusted to roughly match the center of the strong absorptions at 1110 and 2020 cm^{-1} while that of the less intense A$_2''$ transition was situated 41 cm^{-1} higher than the 2020 cm^{-1} band. Centrifugal distortion and first-order Coriolis parameters were calculated with the Asym40 normal coordinate program of Hedberg and Mills,[17] using as input the Cartesian coordinates and force constants obtained from Gaussian at the Hartree$-$Fock level. The vibration$-$rotation coupling constants α_i were also calculated for the normal modes, but these values are believed to be too small due to neglect of anharmonicity. Accordingly, a single, larger, value of $\alpha_A = \alpha_B = 2\alpha_C = -0.0004$ cm^{-1} was taken as representative for all modes, based on α_i values for comparable modes in the somewhat similar molecule cyclopropane.

The calculated parameters are listed in Table 3, and in Figure 3 the simulations for 300 K (b) are compared with experiment

(a). The simulated traces in these figures show that rotational structure in these branches should be easily resolved, a conclusion that is unchanged for reasonable changes in the parameter estimates. Especially, the P$-$Q$-$R branch contours are clearly discernible, in marked contradiction to the observations; thus, other sources of spectral congestion must be considered.

Hot Band Contributions to Spectral Congestion. The ab initio calculations for Al(BH$_4$)$_3$ predict that five of the vibrational modes lie below 500 cm^{-1} and hence less than 10% of the molecules will be in the ground state at room temperature. In particular, an E$'$ type bridge-bending vibration is predicted at 116 cm^{-1} so that the $\nu = 1$ level of this mode, due to its degeneracy, will be more populated than the A$_1'$ ground state. Overtone and combination levels of this mode and other low-frequency modes will lead to many overlapping hot bands, each with small, unknown shifts due to anharmonicity. Such hot band transitions could well blur the rotational contours of the vibrational transitions, as would extensive K splitting of high J rotational lines. Both effects would be greatly reduced at low temperatures; accordingly, several experiments were done in which aluminum borohydride was expanded in a free jet and probed by high-resolution diode laser spectroscopy.

Diode Laser Spectra of Al(BH$_4$)$_3$ Cooled in a Jet. The samples consisted of a 1% mix prepared by flowing argon at 500 Torr through a glass tube containing liquid Al(BH$_4$)$_3$ at about -50 °C (5 Torr vapor pressure). From other work with the PNNL jet apparatus, such conditions are known to produce mainly monomeric samples with rotational temperatures of about 10 K. At these conditions the collisional width will be negligible, and the Doppler width will be less than 0.001 cm^{-1}, the resolution of the diode sources. A typical line width measured with this apparatus for isolated lines of other molecules is 0.002 cm^{-1} fwhm.[13]

The strong absorptions located around 2030 and 1110 cm^{-1} were logical choices for this diode study because they were in regions of available laser sources and there were few overlapping bands of water or diborane that might complicate the spectrum. That appreciable absorption by the Al(BH$_4$)$_3$ occurred in the jet was confirmed by observing the transmitted laser intensity at 2030 cm^{-1} during the jet pulse and also with it turned off. A sharp dip indicated a transmission drop to about 50%. For comparison, in an expansion of pure argon the drop was only 1$-$5%$-$an effect attributed to beam steering by the varying index of refraction caused by the gas pulse. That the dip depends on the laser wavelength is shown by the reduced absorption when the laser was tuned to 2189 cm^{-1}, well off the strong Al(BH$_4$)$_3$ absorption in the region. Coarse I/I_0 traces of the absorption profiles at 2030 and 1110 cm^{-1} were generated in this manner and are shown in Figure 3c, along with the simulated spectra for 10 K for both regions (Figure 3d). A general narrowing of each absorption band is apparent in both jet and simulated spectra.

The diode laser was next scanned over selected 0.4 cm^{-1} portions of these absorption profiles, and representative traces at 2020 and 1110 cm^{-1} are shown at the bottom of Figure 4. It should be noted from the transmission scale of the experimental spectra that the small variations in intensity rest on a broad, nearly continuous absorption background. In the 1110 cm^{-1} region, some structure of very fine regular periodicity is seen that is attributed to an etalon effect in the multipass cell. There is also present both in this spectrum and in the 2020 cm^{-1} scan some evidence of complex overlapping features that are believed to be real. Nonetheless, agreement with the well-resolved, sharp absorptions of the E$'$ Q branch spectra simulated for 10 K is
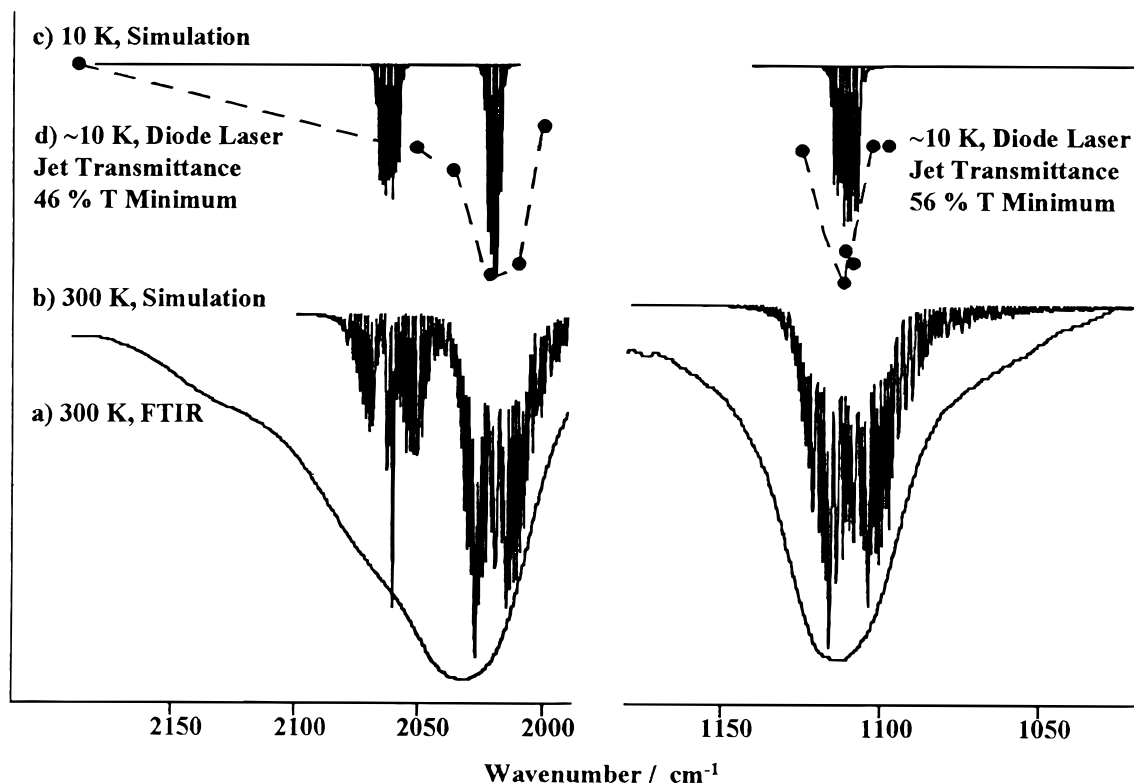
Figure 3. Al(BH$_4$)$_3$ FTIR transmittance regions of interest are expanded in this figure. (a) A 300 K scan at 0.01 cm^{-1} resolution. (b) Simulation for nonrigid rotor at 300 K using parameters in Table 3 and Gaussian line shapes with 0.015 fwhm. Simulations include Al(^{11}BH$_4$)$_3$ (51%) and Al(^{11}BH$_4$)$_2$^{10}BH$_4$ (38%) and the relative ab initio IR intensities. The feature at 2030 cm^{-1} is composed of a parallel band at 2061 cm^{-1} and a perpendicular band at 2020 cm^{-1}. The band at 1110 cm^{-1} is a perpendicular band. (c) Transmittance measurements dotted across each region show a narrowing of the bands in the jet expansion. The temperature is believed to be ~10 K. (d) Simulation at 10 K for Gaussian lines with 0.002 cm^{-1} fwhm.
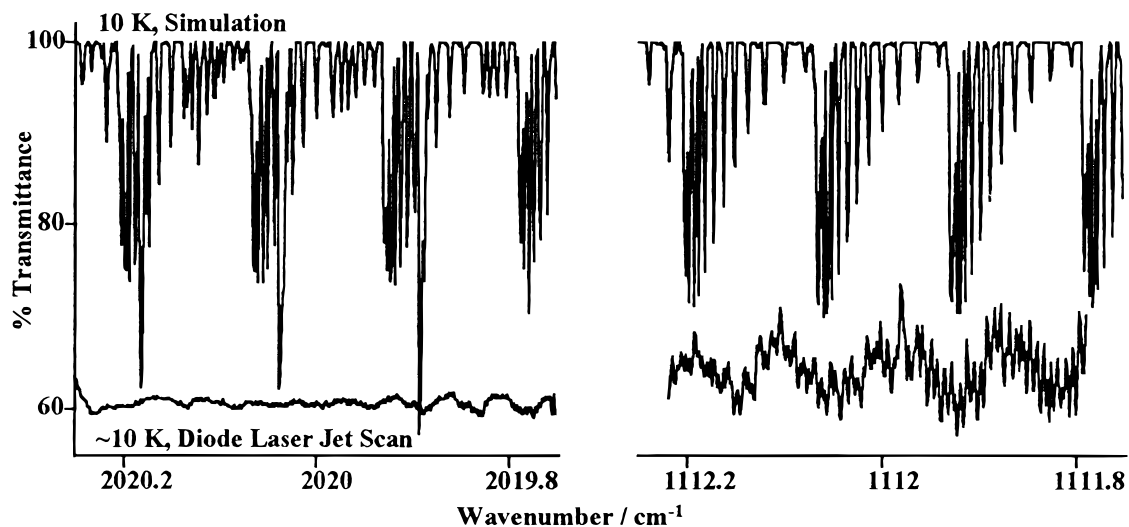
Figure 4. Infrared diode laser spectra of Al(BH$_4$)$_3$ in a supersonic jet expansion are shown in comparison to the simulated pattern of lines for the Q branches of both perpendicular bands. The 100% transmittance level is common for both experimental and simulated spectra for the 1112 cm^{-1} region; in the 2020 cm^{-1} region, the 100% transmittance line for the experimental trace is an estimate.

remarkably poor and is not improved with modest changes in the spectral parameters or the sample temperature.

It is possible that the broad spectral contours in Al(BH$_4$)$_3$ are a consequence of line broadening due to fast internal vibrational relaxation (IVR) of sharp vibration−rotational states that are anharmonically coupled to a high density of background states. Such IVR effects have been seen for some high fundamental and overtone levels and are thought to be enhanced in molecules with torsional motions, as discussed by Lehman et al.[18] For example, high-resolution jet studies of vibration−

rotational line widths for the fundamental acetylenic CH stretch yield lifetimes of 200, 40, 2000, and 850 ps in (CH$_3$)$_3$CCCH, (CD$_3$)$_3$CCCH, (CH$_3$)$_3$SiCCH, and (CD$_3$)$_3$SiCCH, respectively.[19] A lifetime of 40 ps corresponds to a line width (fwhm) of 0.13 cm^{-1}, an amount that could produce the near continua we see in the small spectral region of Figure 4. This would not be sufficient, however, to blur the overall P−Q−R rotational contours to the extent seen in the room temperature spectra of Figure 3. It also seems unlikely that the density of states could be so uniformly high that lifetime broadening would occur

TABLE 3: Rotational Parameters (cm^{-1}) of the Most Abundant Isotopes of Al(BH$_4$)$_3$

rotational parameter[a]	Al^{11}B$_3$H$_{12}$	Al^{10}B^{11}B$_2$H$_{12}$
A''	0.1443	0.1505
B''	0.1443	0.1443
C''	0.0764	0.0778
D_J''	1.82E−7[b]	1.88E−7
D_{JK}''	−3.36E−7	−3.48E−7
D_K''	9.34E−8	9.30E−8
ζ_{17}	1.79E−2	1.80E−2
ζ_{19}	9.48E−3	8.84E−3

[a] Based on HF/6-311G** results and ASYM40. In addition to these constants a vibration−rotation coupling constant of $\alpha_A = \alpha_B = 2\alpha_C = -0.0004$ cm^{-1} was assumed for all modes for the spectral simulations. [b] Read as 1.82×10^{-7}.

throughout the entire vibrational regions shown in Figures 2 and 3. It is of course conceivable that the coupling of the BH$_4$ torsional and tumbling motions with the other internal modes is exceptionally large so that the lifetime shortening is especially pronounced in the metal borohydrides. However, arguing against this is the fact that, in recent jet studies of Be(BH$_4$)$_2$, we have observed a complex pattern of sharp lines in the BH bridge stretch region for which the widths are about 0.003 cm^{-1}, close to the experimental resolution. In this compound, then, the upper state lifetimes are at least 2 ns, and it seems unlikely that this would be shortened by 2 or more orders of magnitude in the aluminum compound.

Rather, we suspect that much of the spectral blurring seen in Al(BH$_4$)$_3$ is due to extreme congestion, even at 10 K. Attribution of this to ineffective quenching of the vibrational hot bands is possible but is considered unlikely because many studies support the idea that (external) vibrational relaxation is very effective in jet expansions.[20,21] Rather, we regard this congestion as a strong experimental indication that the large-amplitude torsion and tumbling motions of Al(BH$_4$)$_3$ play an important role in splitting and distorting the vibrational levels. That such might be the case is suggested by the low ab initio barriers cited earlier, and this has led us to explore in more detail the potential energy surface and its effect on the spectrum.

Potential Energy Calculations. Ab initio calculations were done using Gaussian 94[22] on a DEC Alpha OSF/1 workstation and also on an Intel Pentium Pro 200 MHz system, which gave equivalent CPU performance. The computational model[23,24] was CCSD/6-311G**// MP2/6-311G** for all geometries of interest, and the harmonic frequencies and Cartesian force constants were calculated at the Hartree−Fock level using the same basis set. The geometry optimizations and analytical frequency calculations were done with no symmetry constraints, and all converged to a D$_3$ structure. The HF/6-311G** geometrical parameters agreed well with those of Demachy et al.,[11] as shown in Table 1. Tables 2 and 3 give the vibrational and rotational parameters deduced from these Hartree−Fock calculations and used in the spectral simulations.

The most facile motion of the BH$_4$ units is expected to be the conrotary twist of all units from one D$_3$ form to the other, corresponding to a reversal in the "blade pitch" of this propeller-like molecule. Accordingly, the potential energy of this torsional motion was completely mapped using a **z**-matrix input to fix all variables while scanning the conrotation angle θ. The other structural parameters were then optimized at the maxima at θ = 0° and 90° via the QST3 transition state searching method.[25] Single-point energies were obtained at the minimum and two maxima using a coupled cluster calculation with single and double substitutions (CCSD). The rest of the potential surface points were then scaled to the CCSD maxima with the minimum
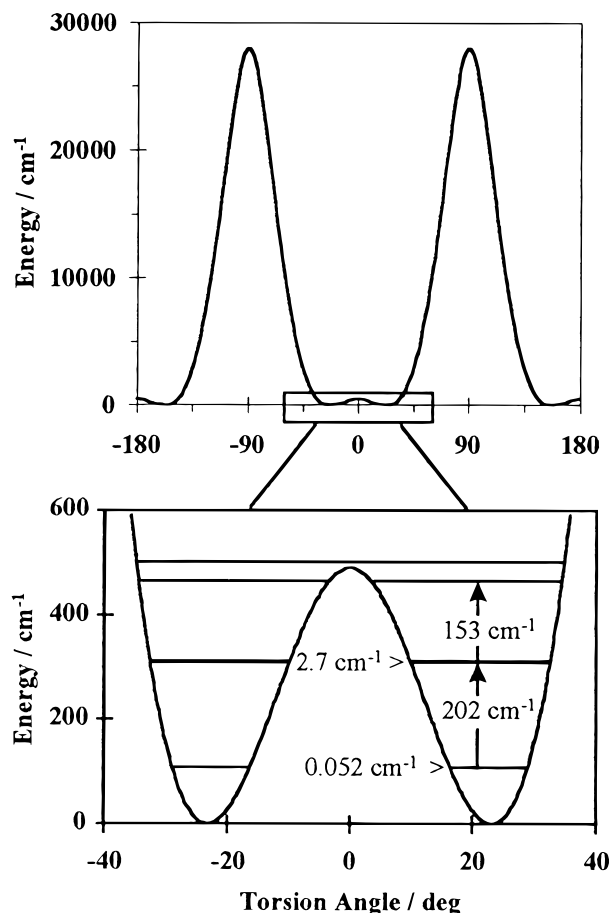
Figure 5. Potential energy of the BH$_4$ torsion (conrotation about the Al−B axes) is periodic with four equivalent minima. The minima separated by the low prismatic barrier (490 cm^{-1}) mix to produce splittings of 0.052 cm^{-1} in the ground state and 2.7 cm^{-1} in the first excited state.

set to zero, and the resulting surface data were fitted with a Fourier series of cosines by least-squares minimization,

$$V(\theta) = V_0 + \sum_{k=2} \frac{V_k}{2}(1 - \cos(k\theta)) \tag{1}$$

An adequate representation of the shape of this torsional potential was obtained for V_k values of $V_0 = 490$ cm^{-1}, $V_2 = 19700$ cm^{-1}, $V_4 = -9150$ cm^{-1}, $V_6 = 1970$ cm^{-1}, and $V_8 = -472$ cm^{-1}, and this function is plotted in Figure 5.

To calculate the effect on the torsional energy levels, the optimized potential function was added to a simple internal rotor Hamiltonian,

$$\hat{H} = \hat{T} + \hat{V} = -\frac{\hbar^2}{2I}\frac{\partial^2}{\partial\theta^2} + V(\theta) \tag{2}$$

where I was taken to be 3 times the moment of inertia of the BH$_4$ unit about the Al−B axis. The matrix elements of this Hamiltonian in a free rotor basis are easily calculated.[26] The resultant matrix was diagonalized numerically using Maple V, and the basis set size was increased until the lowest 12 energy levels converged within 0.0001 cm^{-1}. The energy levels are overlaid with the potential at the bottom of Figure 5 to show the splitting pattern near the minima. A correlation diagram (Figure 6) of the torsional energy levels shows the ground and first two excited states as the prismatic barrier increases from

IR Studies of Al(BH$_4$)$_3$ and Al(BD$_4$)$_3$

J. Phys. Chem. A, Vol. 102, No. 3, 1998 **543**
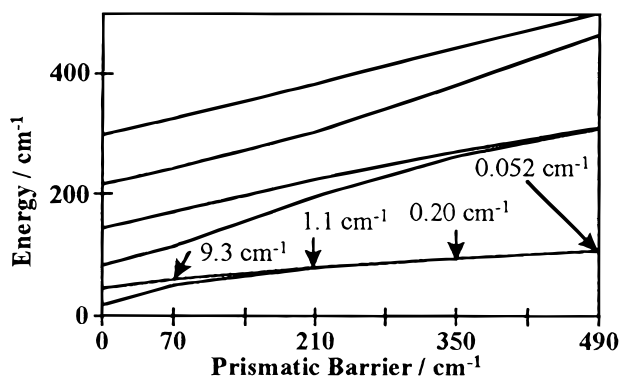
Figure 6. Torsional energy level pattern as the prismatic barrier is increased from zero up to our value of 490 cm^{-1}. The ground-state splitting is 27 cm^{-1} with no barrier, 9.3 cm^{-1} with Demachy et al.'s value of 70 cm^{-1}, and 0.052 cm^{-1} at 490 cm^{-1}.

zero to our calculated value of 490 cm^{-1} (5.9 kJ mol^{-1}). For the latter case, the ground-state splitting is 0.052 cm^{-1}, a value that increases to 2.7 and 36 cm^{-1} for the next two levels, respectively. These splittings of course increase as the prismatic barrier is lowered. For example, a ground-state splitting of 9.3 cm^{-1} is predicted for Demachy et al.'s 70 cm^{-1} (0.8 kJ mol^{-1}) barrier.

Although the validity of these ab initio barrier heights is difficult to assess, it seems clear that the effect of the conrotary torsional motion is enough to cause appreciable splitting of the ground state, thereby producing a doubling of the spectral congestion, even at 10 K. Further splittings can be expected from the other tumbling motions. For the D_{3h} geometry of Al-(BH$_4$)$_3$, there are $(4 \times 3)^3$ equivalent configurations produced by simple rotation of the BH$_4$ units, and hence there will be 1728 states for each rigid rotor vibrational state. These will be retained for a distortion to D_3 symmetry but with doubling of all levels due to the two equivalent minima corresponding to the $\pm$ conrotary twist of all three BH$_4$ units. These states can be classified according to their symmetries in the permutation inversion group formed from all feasible permutations of identical nuclei, with appropriate account taken of the correct combinations with rotational and nuclear spin functions.[27] This group is large, and since no rotational features were resolved, more detailed symmetry analysis does not seem warranted. We note however that the number of rotational symmetries will be small and cyclic, repeating for $K = 3p$, $3p \pm 1$ with p an integer. Each K value will correspond to many nuclear spin symmetries that will not interconvert in the expansion but which cannot be distinguished beyond this K grouping.

The extent to which sublevel splittings are discernible for this manifold of states will depend upon the ease of internal BH$_4$ rotation that produces the hydrogen interchange. In the case of LiBH$_4$, microwave rotational spectra[28] show no ground-state splittings attributable to mixing of the 12 equivalent states separated by the tumbling barrier. This splitting is estimated at 6.3×10^{-5} cm^{-1} by Baronov and Boldrev,[29] based on their ab initio value of 1053 cm^{-1} for the tumbling barrier. A somewhat lower, but still appreciable, barrier of 770 cm^{-1} has been calculated for Al(BH$_4$)$_3$ by Demachy et al. so that the splittings in the ground state due to tumbling exchanges would be expected to be very small in this molecule as well. Such will not be the case for higher tumbling levels, however, as illustrated by the calculations above for the conrotary torsional mode.

The higher vibrational levels most susceptible to splitting by tumbling motion will involve the BH$_4$ rocking, wagging, and twisting modes that combine to produce the tumbling coordinates. Although the three bands examined in our jet measurements are believed to consist primarily of BH$_2$ deformation and BH bridge stretching coordinates, in the normal modes there will be mixing to some extent with tumbling coordinates of common symmetry. In addition, anharmonic coupling via Fermi resonance with overtone and combination levels involving torsional and tumbling modes can separate sublevels of different symmetry even when the normal mode coupling is small. For example, in ethane, we have recently observed Fermi resonance between the CC stretch and the fourth torsional overtone, resulting in separation of the six upper state torsional sublevels by up to 1 cm^{-1}.[20] Only by proper account of this Fermi interaction and the state symmetries and nuclear spin restrictions was the spectrum interpretable. Given the number of torsional and tumbling modes in Al(BH$_4$)$_3$, such resonant perturbations, along with other effects discussed above, are likely to be important and to contribute to the extreme spectral congestion that this unusual molecule displays.

Conclusions

We have obtained very high-resolution IR spectra of Al(BH$_4$)$_3$ that show no resolved rotation−vibrational structure, even at the low temperatures achieved in a cold jet. The possibility of line broadening by IVR processes exists but is not believed to be the dominant factor. Rather, ab initio calculations suggest that extreme spectral congestion may arise from small isotopic shifts due to ^{10}B, many low-frequency modes below 500 cm^{-1}, and especially level splittings due to low barriers to internal rotation. The Al(BH$_4$)$_3$ molecule is a prime example of the complexity introduced by equivalent structural minima and large-amplitude motions, a situation often met in the case of van der Waals complexes but less commonly for covalently bonded molecules. The metal borohydrides thus represent an unusual class of compounds in which ionic interactions appear to hold together BH$_4^-$ units that have large librational motion. Such motions have recently been considered in analyzing the microwave rotational spectra of the alkali metal borohydrides, and studies of the vibration−rotational spectra of LiBH$_4$ and of Be(BH$_4$)$_2$ would seem worthwhile, particularly for samples cooled in a jet.

References and Notes

(1) Almenningen, A.; Gundersen, G.; Haaland, A. *Acta Chem. Scand.* **1968**, *22*, 328.

(2) Coe, D. A.; Nibler, J. W. *Spectrochim. Acta* **1973**, *29A*, 1789.

(3) Plato V.; Hedberg K. *Inorg. Chem.* **1971**, *10*, 590. James B. D.; Wallbridge, M. G. H. *Prog. Inorg. Chem.* **1970**, *11*, 99.

(4) Schlesinger, H. I.; Brown, H. C.; Burg, A. B. *J. Am. Chem. Soc.* **1940**, *62*, 3421.

(5) Beach, T. Y.; Bauer, S. H. *J. Am. Chem. Soc.* **1940**, *62*, 3440.

(6) Ogg, R. A.; Ray, J. D. *Discuss. Faraday Soc.* **1955**, *19*, 215.

(7) Maybury P. C.; Ahnell, J. E. *Inorg. Chem.* **1967**, *6*, 1286.

(8) Price, W. C. *J. Chem. Phys.* **1949**, *17*, 1044.

(9) Emery, A. R.; Taylor, R. C. *Spectrochim. Acta* **1960**, *16*, 1455.

(10) Bock, C. W.; Roberts, C.; O'Malley, K.; Trachtman, M.; Mains, G. J. *J. Phys. Chem.* **1992**, *96*, 4859.

(11) Demachy, I.; Volatron, F. *Inorg. Chem.* **1994**, *33*, 3965.

544 *J. Phys. Chem. A, Vol. 102, No. 3, 1998*

Al-Kahtani et al.

(12) Schlesinger, H. I.; Brown, H. C.; Hyde, E. K. *J. Am. Chem. Soc.* **1953**, *75*, 209.

(13) Sharpe, S. W.; Zeng, T. P.; Wittig, C.; Beaudet, R. A. *J. Chem. Phys.* **1990**, *92*, 943.

(14) Foresman, J. B.; Frisch, Æ. *Exploring Chemistry with Electronic Structure Methods*, 2nd ed.; Gaussian Inc.: Pittsburgh, PA, 1996; p 64.

(15) Grams/32 Spectral Notebase, Galactic Industries Corp.

(16) Allen, Jr., H. C.; Cross, P. C. *Molecular Vib-Rotors*; John Wiley and Sons: New York, 1963.

(17) Hedberg, L.; Mills, I. M. *J. Mol. Spectrosc.* **1993**, *160*, 117.

(18) Lehmann, K. K.; Scoles, G.; Pate, B. H. *Annu. Rev. Phys. Chem.* **1994**, *45*, 241.

(19) Gambogi, J. E.; L'Esperance, R. P.; Lehmann, K. K.; Pate B. H.; Scoles, G. *J. Chem. Phys.* **1993**, *98*, 1116.

(20) Al-Kahtani, A.; Montero, S.; Nibler, J. W. *J. Chem. Phys.* **1993**, *98*, 101.

(21) Van Helvoort, R.; Knippers, W.; Fantoni, R.; Stolte, S. *Chem. Phys.* **1987**, *111*, 445.

(22) Gaussian 94, Revision E.1: Frisch, M. J.; Trucks, G. W.; Schlegel, H. B.; Gill, P. M. W.; Johnson, B. G.; Robb, M. A.; Cheeseman, J. R.; Keith, T.; Petersson, G. A.; Montgomery, J. A.; Raghavachari, K.; Al-Laham, M. A.; Zakrzewski, V. G.; Ortiz, J. V.; Foresman, J. B.; Cioslowski, J.; Stefanov, B. B.; Nanayakkara, A.; Challacombe, M.; Peng, C. Y.; Ayala, P. Y.; Chen, W.; Wong, M. W.; Andres, J. L.; Replogle, E. S.; Gomperts, R.; Martin, R. L.; Fox, D. J.; Binkley, J. S.; Defrees, D. J.; Baker, J.; Stewart, J. P.; Head-Gordon, M.; Gonzalez, C.; Pople, J. A. Gaussian, Inc., Pittsburgh, PA, 1995.

(23) Møller, C.; Plesset, M. S. *Phys. Rev.* **1934**, *46*, 678.

(24) Scuseria, G. E.; Schaefer, III, H. F. *J. Chem. Phys.* **1989**, *90*, 3700.

(25) Peng, C.; Schlegel, H. B. *Isr. J. Chem.* **1993**, *33*, 449.

(26) Flygare, W. H. *Molecular Structure and Dynamics*; Prentice-Hall: Englewood Cliffs, NJ, 1978; Section 4.2.

(27) Ohashi, N.; Hougen, J. T. *J. Mol. Spectrosc.* **1992**, *153*, 429.

(28) Hirota, E.; Kawashima, Y. *J. Mol. Spectrosc.* **1997**, *181*, 352.

(29) Baranov, L. Ya.; Boldyrev, A. I. *Chem. Phys. Lett.* **1983**, *96*, 218.